What Should You Know? A Human-In-the-Loop Approach to Unknown Unknowns Characterization in Image Recognition

Shahin Sharifi Noorian, Sihang Qiu, Ujwal Gadiraju, Jie Yang* and Alessandro Bozzon
{s.sharifinoorian,s.qiu-1,u.k.gadiraju,j.yang-3,a.bozzon}@tudelft.nl
Delft University of Technology
Delft, The Netherlands

ABSTRACT

Unknown unknowns represent a major challenge in reliable image recognition. Existing methods mainly focus on unknown unknowns identification, leveraging human intelligence to gather images that are potentially difficult for the machine. To drive a deeper understanding of unknown unknowns and more effective identification and treatment, this paper focuses on unknown unknowns characterization. We introduce a human-in-the-loop, semantic analysis framework for characterizing unknown unknowns at scale. We engage humans in two tasks that specify what a machine *should know* and describe what it *really knows*, respectively, both at the conceptual level, supported by information extraction and machine learning interpretability methods. Data partitioning and sampling techniques are employed to scale out human contributions in handling large data. Through extensive experimentation on scene recognition tasks, we show that our approach provides a rich, descriptive characterization of unknown unknowns and allows for more effective and cost-efficient detection than the state of the art.

CCS CONCEPTS

• **Computing methodologies** → **Machine learning**; **Knowledge representation and reasoning**; • **Human-centered computing** → **Human computer interaction (HCI)**.

KEYWORDS

Unknown unknowns, humans in the loop, semantic analysis

ACM Reference Format:
Shahin Sharifi Noorian, Sihang Qiu, Ujwal Gadiraju, Jie Yang* and Alessandro Bozzon. 2022. What Should You Know? A Human-In-the-Loop Approach to Unknown Unknowns Characterization in Image Recognition. In *Proceedings of the ACM Web Conference 2022 (WWW '22), April 25–29, 2022, Virtual Event, Lyon, France.* ACM, New York, NY, USA, 11 pages. https://doi.org/10.1145/3485447.3512040

1 INTRODUCTION

Machine learned image recognition models are rapidly deployed in many high-stakes contexts [35]. While largely accelerating and aiding the decision-making process, such models suffer from a severe issue of reliability—they can just as easily fail and generate errors that can eventually lead to drastic consequences [41]. Being able to understand and detect such errors has become a key demand for both, model developers to debug and improve the model [4], and for the users to decide when to trust the model output [11, 12, 50].

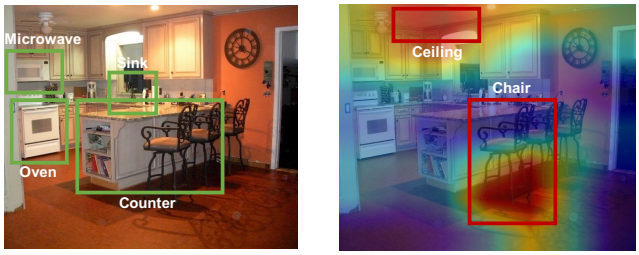

(a) SHOULD-KNOW Specification (b) REALLY-KNOWS Description

Figure 1: An unknown unknown example: Kitchen image classified as Conference Room. The model misses relevant concepts *microwave*, *oven*, *counter* and *sink* specified in (a) what the model should know, while picking up irrelevant concepts *chair* and *ceiling* shown in (b) what the model really knows (based on the saliency map [46]).

Among image recognition errors, a specific type known as *unknown unknowns* is of particular interest [5, 29]. Unknown unknowns refer to the images for which a model is highly confident about its predictions but is wrong. Identifying such errors is challenging due to the overconfidence of the model. Recent efforts resort to *human-in-the-loop* approaches that ask humans to gather data instances that are potentially difficult for a model to handle [5, 27, 29]. An important finding reveals that unknown unknowns often come with internal consistency, making them particularly suitable to be described by natural language building on top of conceptual knowledge [5, 17, 29]. We bring to fore the notion of *characterizing* unknown unknowns to allow us to gain a deeper understanding of when the model fails. This lies in contrast to previous work that has focused largely on *identifying* unknown unknowns.

For effective characterization of unknown unknowns, two types of knowledge are needed: knowledge of what a model *has learned*, that we henceforth refer to as REALLY-KNOWS, and what a model *should have learned*, referred to as SHOULD-KNOW. Recent work on human-in-the-loop machine learning interpretability [6] has shown the important role of humans as computational agents to describe REALLY-KNOWS, by annotating salient image areas in image recognition with semantic concepts. In this paper, we advocate another view to the role of humans as contributors who can shed light on SHOULD-KNOW. We envision that eliciting SHOULD-KNOW from the perspective of human understanding of a given task, can lead to a complete and usable characterization of unknown unknowns. Consider the example of indoor scene recognition in Figure 1, where the model incorrectly classifies a Kitchen image as a Conference

* Corresponding author.

WWW '22, April 25–29, 2022, Virtual Event, Lyon, France

ACM ISBN 978-1-4503-9096-5/22/04.
https://doi.org/10.1145/3485447.3512040

Room: knowing that the model fails by focusing on the *chair* and *ceiling* only tells half the story; knowing that the model should have focused on the *microwave*, *oven*, *counter*, for instance, presents a deeper understanding that would allow further identification of similar errors which the model produces by missing such concepts.

With this in mind, we introduce **Scalpel-HS**, a human-in-the-loop, semantic analysis framework for unknown unknowns characterization in image recognition. Drawing inspiration from cognitive psychology literature [16, 20, 30, 36], **Scalpel-HS** is designed with two human computation tasks— for SHOULD-KNOW specification and REALLY-KNOWS description—that both engage human contributors to operate at the conceptual level. In the SHOULD-KNOW task, human contributors identify a set of objects (with attributes) and relations that are relevant for a given image. In the REALLY-KNOWS task human contributors annotate areas of an image, shown to be relevant for model prediction, with semantic concepts (i.e., visual objects, attributes, and relations). Leveraging the outcome from both SHOULD-KNOW and REALLY-KNOWS tasks, model unknowns can be characterized by comparing those concepts that a model should have learned with what the model actually learned.

Scalpel-HS builds upon a computational pipeline to provide input to the human computation tasks with minimized cognitive load imposed to human contributors. For the SHOULD-KNOW task, we leverage state-of-the-art information extraction techniques to pre-identify objects and relations in the images, allowing human contributors to primarily focus on adjudicating the relevance of concepts to a given scene. This cognitively simplifies the task at hand, in comparison to explicitly synthesizing relevant concepts [25], and results in a more structured vocabulary. For the REALLY-KNOWS task, we leverage machine learning interpretability methods to highlight important pixels of an image for model prediction [45, 46]. To minimize human effort, **Scalpel-HS** employs a semantic data partitioning and sampling method that identifies representative images for the human tasks. To do so, **Scalpel-HS** starts off by first learning semantically-rich image representations.

We demonstrate the effectiveness, informativeness, and cost-efficiency of **Scalpel-HS** on several state-of-the-art machine learning models for scene recognition [26, 55], a task that is considered to be complex in image recognition for machines, as well as for humans as it requires the understanding of context [31, 54]. We show that **Scalpel-HS** provides informative, easy-to-understand characterizations of unknown unknowns that significantly boost the state of the art in unknown unknown detection by *31%*, and is able to detect *2x to 3x* the sizes of unknown unknowns compared to the number of annotated images.

In summary, we make the following key contributions:

- We introduce a human-in-the-loop framework that orchestrates both automatic and human computation components for cost-efficient characterization and identification of unknown unknowns;
- We present the design of human computation tasks for both model should-know and actually-knows description at the conceptual level, with a set of design choices made to account for the cognitive load, and fault-tolerance of human work;
- We introduce computational methods for learning semantically rich image representations and for image sampling by partitioning the semantic data space, for scaling out human contributions.

2 THE SCALPEL-HS FRAMEWORK

Figure 2 presents an overview of **Scalpel-HS**. Given an image set and a trained image recognition model, it first 1a extracts the scene graphs of the images and 1b the saliency maps for the model classification of the given images. It 2a learns the representation of the images combining both the visual and semantic features and based on that, 2b partitions the image set and sample representative images for the human tasks. The scene graphs and the saliency maps of the sampled images are then respectively fed to the human tasks published in a crowdsourcing platform, 3a the SHOULD-KNOW task, and 3b the REALLY-KNOWS task, to generate descriptions of what a model should know and really knows. Output of the two tasks are then aggregated to obtain a characterization of the unknown unknowns, together with a set of corresponding unknown unknown images through the 4 aggregation and detection component.

In the following, we describe the components in more detail.

1a Scene Graph Extraction. Understanding a natural scene image usually requires reasoning about the relationship between objects in the image. For example, in the recognition of rooms, a sink next to an oven indicates a kitchen while a sink next to a mirror more likely indicates a bathroom. To help humans specify the required knowledge in scene recognition, i.e., SHOULD-KNOW, we extract scene graphs. A scene graph is a structured representation of objects and the relationships between them present in an image. It consists of a set of relationships, each represented as $[o_i, r_{ij}, o_j]$, where o_i and o_j refer to two objects (image patches usually captured by bounding boxes) in the image, and r_{ij} represents the relation between two objects. Given a scene image, we generate the visual scene graph using state-of-the-art methods Neural Motifs [53].

1b Saliency Map Extraction. Understanding machine behavior in scene recognition is the machine learning interpretability problem. The most extensively studied interpretability approach for image classification is saliency, a local interpretability post-hoc method that highlights the most important pixels of an image for model decisions in what is called a saliency map [45]. We choose this method to help humans describe what a model REALLY-KNOWS.

We opted for SmoothGrad [46], which is sensitive to the parameters of a model (thus catering for more accurate capturing of a model behavior) while minimizing noisy results (i.e., highlighting irrelevant pixels). Our framework is though agnostic to the employed local interpretability method. To minimize human effort, we sample a subset of representative images for human annotation. Data sampling is performed via a data partitioning method based on a new type of image representation.

2a Representation Learning. Due to the complexity of the scene recognition task, representative images should be diverse in terms of both the semantic information contained and the visual appearance. Existing methods generally rely on pre-trained models for visual feature extraction only, which is suboptimal in our context. We propose to fuse in also the semantic information and introduce a self-supervised learning approach for learning semantically rich image representations. We describe the details in Section 3.1.

2b Data Partitioning and Sampling. Prior work has shown that unknown unknowns are caused by systematic biases in training data, reside in certain partitions (i.e., blind spots) of the feature

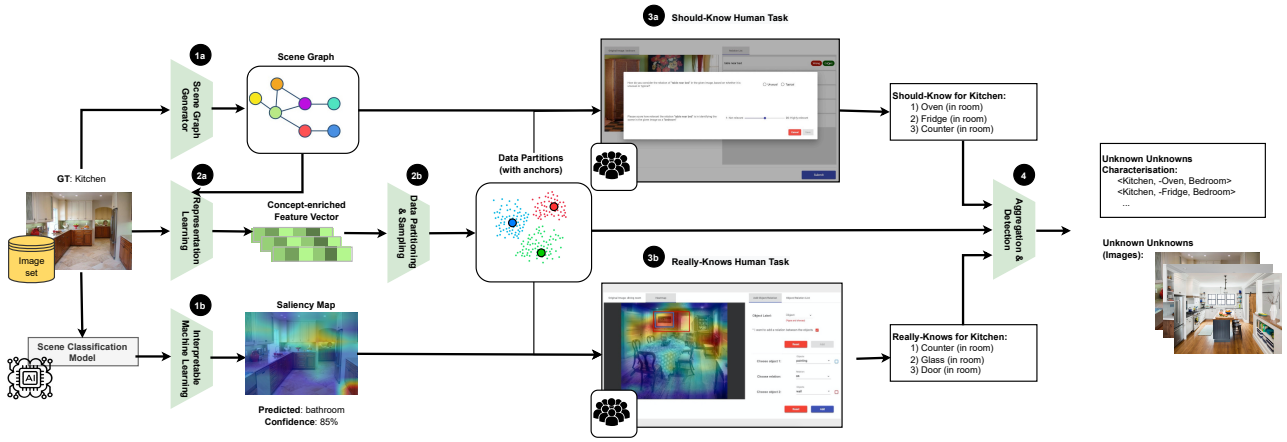

Figure 2: The `Scalpel-HS` framework. It takes as input an image set and a trained image recognition model; as output, it produces a characterization of unknown unknowns and identifies the corresponding unknown unknown images. To do so, it extracts the (1a) scene graph and (1b) saliency map of model classification of a subset of images—sampled by (2a) representation learning and (2b) data partitioning—, feeds them to the (3a) `SHOULD-KNOW` and (3b) `REALLY-KNOWS` human computation tasks published on a crowdsourcing platform, and (4) aggregates the output for unknown unknowns characterization and detection of more corresponding unknown unknown images.

space [5, 29]. Following this, we propose a data partitioning method for sampling, *Semantic Space Partitioning (SSP)*, that identifies the optimal subset of representative images in the semantic space. Our method partitions the semantic space and selects candidate images in such a way that (the weighted sum of) cosine distances from the candidate data points to others in the same region are minimized. As the result, semantically similar images will be grouped in partitions, centered around the representative images. Those representative images are then sampled for human annotations. We describe the details of our SSP method in Section 3.2.

3a The `SHOULD-KNOW` Task. For a given set of valid objects and relations pertaining to a scene, it is important to understand the salience of each object and relation in identifying the scene in the given image. For example, from a human perspective, a `bed` when compared to a `carpet` can be deemed to be relatively more salient in identifying the scene as a `bedroom`. In this task, human workers identify the salient objects, their attributes, and the relations between objects for identifying a given scene in an image. We describe details of the task design in Section 4.1.

3b The `REALLY-KNOWS` Task. The goal of the task is to find out which objects in the scene influence the prediction of the machine learning model, and whether this is congruent with the human mental model. Human workers identify objects and relations found by the machine, and rate their relevance in identifying the scene. Details of the task are described in Section 4.2.

4 Aggregation & Detection. Results of the two human tasks are aggregated to obtain a characterization of unknown unknowns. Denoting the true class and wrongly predicted class as y and y', respectively, the characterization is represented in the form of the triple $\langle y, (+)c, y' \rangle$ for False Positive (in terms of y') and $\langle y, (-)c, y' \rangle$ for False Negative (in terms of y). For example, $\langle$`Conference Room`, $(+)$*sofa*, `Living Room`$\rangle$ indicates that the model wrongly classifies a conference room image to be a living room because of the focus on the spurious concept sofa; $\langle$`Kitchen`, $(-)$*oven*, `Conference Room`$\rangle$ indicates that the model wrongly classifies a kitchen image to be a conference room by missing the concept of oven in the kitchen.

Apart from the characterization, this component detects more unknown unknowns of the same characteristics utilizing the data partitions: images in the same partition as the human annotated (representative) one are likely to be unknown unknowns sharing the same missing or spurious concepts. The component therefore, identifies more images as unknown unknowns those on which the model confidence is greater than a threshold.

3 IMAGE REPRESENTATION AND SAMPLING

This section describes our methods for semantically rich image representation learning and semantic space partitioning.

3.1 Representation Learning

Our representation learning model comprises components for visual feature extraction, semantic feature extraction, multi-modality fusion, and image representation generation. Together those components make a representation learning model that can be trained in an end-to-end fashion. We describe the details in the following.

Visual Feature Extraction. We use the pre-trained model Faster-RCNN [38] to generate feature vectors for nodes and relationships in the generated scene graph. For each object node o_i in the scene graph, a visual feature vector $\mathbf{V}_{o_i}$ is extracted from its corresponding image region. For each relationship node r_{ij}, its visual feature vector $\mathbf{V}_{r_{ij}}$ is extracted from the union region of o_i and o_j on the image.

Semantic Feature Extraction. Each node, either object node or relationship node, has a text description generated by the scene graph generator. From such text description, we obtain the initial semantic features using the pre-trained GloVe embeddings [34]. Those embeddings are trainable parameters in our representation method. We denote the semantic feature of the node and relationship as $\mathbf{E}_{o_i}$ and $\mathbf{E}_{r_{ij}}$, respectively.

Multi-modality Fusion. We fuse the visual and semantic features into a joint multi-modal representation. Inspired by [18], the visual

feature vector and label feature vector are first concatenated, then fused as follows:

$$\mathbf{Z}_{o_i} = \tanh(\mathbf{W}_1^T \mathbf{V}_{o_i} + \mathbf{W}_2^T \mathbf{E}_{o_i}) \quad (1)$$

$$\mathbf{Z}_{r_{ij}} = \tanh(\mathbf{W}_1^T \mathbf{V}_{r_{ij}} + \mathbf{W}_2^T \mathbf{E}_{r_{ij}}) \quad (2)$$

where $\mathbf{Z}_{o_i}$ and $\mathbf{Z}_{r_{ij}}$ are joint feature vectors for object and relation nodes, respectively. $\mathbf{W}_1$ and $\mathbf{W}_2$ are the shared parameters.

Image Representation Generation. To obtain a single vector representation of an image, we combine the visual-semantic features of all the objects and relationships. Considering the fact that those objects and relations together make a graph, we employ a multi-layer graph convolutional networks (GCN) [24] to capture the graph structure while combining the object and relationship features. Through multiple layers of linear and non-linear transformation layers, GCN generates new node features that contain structural information of the graph. To obtain a global representation of the image, we aggregate the node representations learned by GCN in different layers—denoted as $\mathbf{U}_{o_i}$ and $\mathbf{U}_{r_{ij}}$ for object and relationship nodes respectively—into a graph representation using a graph pooling operation, known as readout [32, 52].

The entire representation learning model contains parameters of embedding, the multi-modality fusion layer, and those of the GCN. We describe the training details in Appendix A.1.

3.2 Semantic Space Partitioning

Formally, we denote the distance between the feature vectors f_i, f_j of two images i, j as following,

$$dist(f_i, f_j) = 1 - \frac{{f_i}^T f_j}{\|f_i\| \|f_j\|}. \quad (3)$$

Given a budget $\mathcal{B}$, i.e., the number of representative images to be sampled for human tasks, our partitioning method finds the representation images by minimizing the following objective function:

$$\begin{aligned} min & \sum_{i \in \mathcal{D}} \sum_{j \in \mathcal{D}} dist(f_i, f_j) X_{ij} \\ s.t. & \sum_{j \in \mathcal{D}} X_{ij} = 1 \\ & X_{ij} \leqslant Y_j \\ & \sum_{j \in \mathcal{D}} Y_j = \mathcal{B} \end{aligned} \quad (4)$$

where X_{ij} indicates the decision of whether image i is assigned to partition j; Y_j indicates if image j is selected as a representative sample (note that the index j is overloaded to represent both the partition and the representative image of the partition).

Due to the large number of possible solutions that are associated with the problem of finding an optimal set of representative samples, it is very challenging to provide a deterministic solution. We employ a meta-heuristic approach based on genetic algorithms (GA). Details of our algorithm are described in Appendix A.2.

4 THE HUMAN COMPUTATION TASKS

We now describe the human computation tasks for specifying what an image recognition model SHOULD-KNOW and what it REALLY-KNOWS.

4.1 The SHOULD-KNOW Task

In this task, human workers are presented with a sampled image, and the corresponding scene graph, to identify concepts (salient objects, their attributes, and relations) in scene recognition. The procedure is shown in Figure 3 (zoomed figures in Appendix A.3). Workers are first asked to (a) validate the automatically generated objects and relations within the scene graph. Erroneous objects and relations can thereby be identified and filtered (Neural Motifs performance in object and relation classification are 33%, 59% respectively [53]). They are then tasked to (b) rate the relevance of concepts in scene recognition using a slider ranging from 1 to 20 (not relevant at all to highly relevant).

To further scope down to the highly relevant concepts, workers are asked to identify the minimum set of concepts that can sufficiently identify the scene. It implicitly requires humans to first (c) add missing concepts, and then (d,e) determine the indispensable concepts for identifying the scene in the given image. To add missing concepts, workers need to specify the concept by entering the name and drawing a bounding box in the image. In the case of the concept being an object attribute or a relationship, the worker needs to further specify the relations. Indispensable concepts are selected using checkboxes from the concept list.

4.2 The REALLY-KNOWS Task

While a scene in the human mind is composed of objects possessing clear boundaries and having intelligible locations in space relative to each other [44], to the machine it is the composition of pixels rather than objects. To understand machine behavior, we map the pixels highlighted in warm colors by the saliency map, to actual concepts that humans can understand. The procedure is shown in Figure 4 (zoomed figures in Appendix A.3). Workers are asked to (a) draw bounding boxes to annotate objects highlighted by the saliency map, (b) name the objects and assign the attributes (e.g., color), (c) define relations among the objects, and (d) add all the objects and relations highlighted by the saliency map to the list.

By comparing to their own mental models in scene recognition, workers then (e) rate the relevance these objects/relations are in identifying the scene, using a slider (ranging from 1 to 20, meaning not relevant at all to highly relevant). They are also encouraged to give reasons. Note that with annotations from this task, a characterization of false positive prediction due to the wrong focus on the spurious concept can already be obtained. We compare in our experiments unknown unknowns detection using only the characterization obtained from this REALLY-KNOWS task and that from also the SHOULD-KNOW task.

5 EXPERIMENTAL SETUP AND RESULTS

We evaluate the performance of **Scalpel-HS** by investigating the following questions[1]: **Q1**: How effective is it in detecting and characterizing unknown unknowns? **Q2**: how informative are those characterization provided by our framework? and **Q3**: how cost-efficient is our framework under a limited budget? For these questions, we further evaluate the contribution of the individual components of **Scalpel-HS** and compare to the state of the art whenever possible.

[1] Source code and data are available at https://sites.google.com/view/www22-scalpel-hs

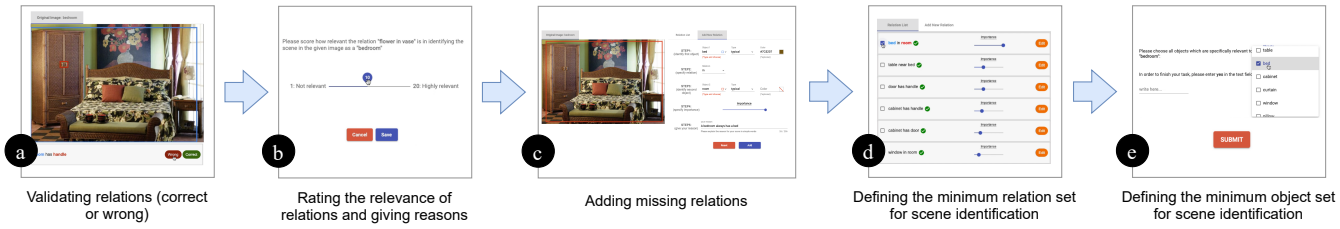

Figure 3: The procedure of the SHOULD-KNOW task for specifying what a model should know in scene recognition. (Zoomed in Appendix A.3)

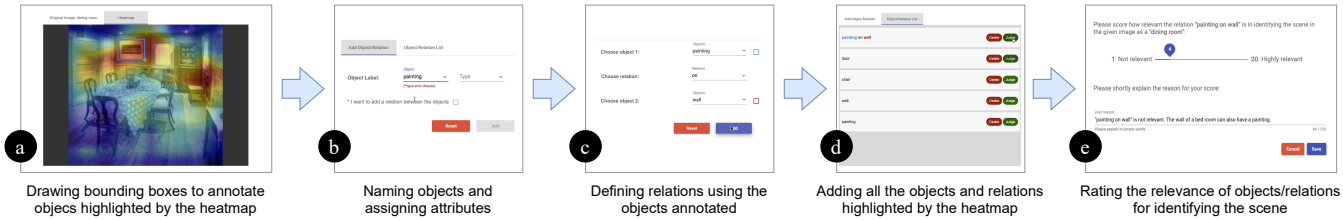

Figure 4: The procedure of the REALLY-KNOWS task for describing what a model really knows in scene recognition. (Zoomed in Appendix A.3)

5.1 Experimental Setup

Datasets. We use two image datasets: (1) *PLACES*: it contains 10 million images divided into over 400 unique scene classes with 5000 to 30,000 training images and over 100 test images per class. As not all classes are about scenes, we select a subset of data containing nine indoor scene classes. (Details provided in the Appendix A.4.) The subset contains 60000 training and 1000 test images equally distributed across the nine classes. (2) *MIT67*: this dataset contains 15620 images in 67 indoor classes. Unlike the PLACES dataset, the number of images varies across classes, however, there are at least 100 images per class. We filter images of the same set of scene classes as PLACES and select a subset consisting of 3224 test images with at least 100 images per class. Note that due to the limited number of images in MIT67, there are only 3216 images left after filtering; we therefore only use the training set of PLACES for model training. Test sets from PLACES and MIT67 allow us to experiment with model unknowns exposed in test data of different distributions.

Unknown Unknowns Creation. We consider the unknown unknowns characterization effective in two senses: it exposes the reasoning of an image recognition model in a high-confidence yet wrong prediction, and it allows for the detection of unknown unknowns images of the same type. Note that while the ground truth labels are given in the test set—hence unknown unknowns images are known by comparing the model output to the ground truth labels—the ground truth of the model reasoning is in-transparent. To cope with this issue, inspired by previous work [6], we bias model reasoning by forcing the model to focus on spurious concepts or to miss relevant concepts through data re-sampling. To do so, we create unknown unknowns of False Positive by removing concepts from training images of all classes except those of the class of interest. By doing so, the model will strongly associate the spurious concept with the class of interest and make wrong predictions for test images of other classes. Similarly, we create unknown unknowns of False Negative by removing concepts from the training images of the class of interest (not other classes). To make sure the concepts are distributed in several classes, we select 15 most frequent concepts (objects and relations) and then those that are distributed across at least three classes. A co-occurrence matrix between concepts and scene classes is provided in the companion page. The induced unknown unknowns are summarized in Table 1.

Table 1: Summary of induced unknown unknowns.

Type	Index	Class of Interest	Concept
False Positive	FP1	Kindergarden	*person*
	FP2	Bedroom	*bed*
	FP3	Conference Room	*chair*
False Negative	FN1	Kitchen	*oven*
	FN2	Bathroom	*sink*
	FN3	Dining Room	*wine glass*
	FN4	Living Room	*couch/sofa*
	FN5	Conference Room	*woman at table*
	FN6	Kindergarden	*boy wearing shirt*

Apart from evaluating the effectiveness of our framework in exposing the incorrect reasoning and in detecting unknown unknowns that are manually induced, we further look into the informativeness of the characterization for "natural" unknown unknowns, i.e., those unknown unknown images without the chosen concepts (or missed by the scene graph extractor). Note that while we cannot make sure that the model makes high-confidence errors on all images with the identified characteristics, we are sure about the errors when they occur given the ground truth labels and about model rationales for images annotated by our framework.

Scene Recognition Models. We conduct our experiment with two state-of-the-art convolution neural networks, ResNet[19] and DenseNet[23], which have shown superior performance on various classification tasks [48]. We train the two scene classifiers for 50 epochs on the biased training data and confirm that biases are successfully injected into the scene classifier by observing overfitting of the performance metrics during the training phase.

Table 2: Performance (P = Precision, R = Recall, and F = F1-score) comparison with baseline methods on detecting unknown unknowns images. We highlight the best performance for each metric in bold.

Type	Comparison Method	ResNet						DenseNet					
		Places			MIT67			Places			MIT67		
		P	R	F	P	R	F	P	R	F	P	R	F
False Positive	Random	0.383	0.187	0.251	0.311	0.158	0.209	0.39	0.161	0.228	0.336	0.120	0.177
	Least Average Similarity	0.558	0.272	0.366	0.318	0.161	0.214	0.558	0.272	0.366	0.663	0.218	0.329
	Least Maximum Similarity	0.379	0.185	0.249	0.232	0.118	0.156	0.379	0.185	0.249	0.616	0.209	0.312
	Most Uncertain	0.348	0.170	0.228	0.44	0.223	0.296	0.351	0.183	0.240	0.53	0.190	0.279
	UUB	0.629	0.378	0.472	0.755	0.383	0.509	0.617	0.394	0.480	0.702	0.282	0.402
	Scalpel-HS	**0.855**	**0.522**	**0.648**	**0.915**	**0.465**	**0.616**	**0.874**	**0.716**	**0.787**	**0.766**	**0.521**	**0.620**
False Negative	Random	0.21	0.08	0.11	0.28	0.152	0.197	0.293	0.271	0.281	0.33	0.09	0.141
	Least Average Similarity	0.542	0.279	0.368	0.663	0.218	0.329	0.542	0.279	0.368	0.589	0.155	0.246
	Least Maximum Similarity	0.372	0.185	0.247	0.616	0.209	0.312	0.372	0.185	0.247	0.495	0.135	0.212
	Most Uncertain	0.585	0.219	0.319	0.452	0.246	0.319	0.549	0.237	0.331	0.44	0.12	0.188
	UUB	0.551	**0.634**	0.589	0.480	0.376	0.422	0.553	0.649	0.597	0.456	0.271	0.340
	Scalpel-HS	**0.711**	0.525	**0.604**	**0.653**	**0.435**	**0.522**	**0.577**	**0.678**	**0.624**	**0.704**	**0.364**	**0.480**

Baseline Methods. Following previous work [27, 29], we compare the performance of our pipeline against the following methods: 1) Random Sampling: Randomly selects instances from the test data to be queried with humans. 2) Least Average Similarity [8]: Computes the average Euclidean distance for each test instance to all training instances, and chooses the instances with the highest distances. 3) Least Maximum Similarity [8]: Computes the minimum Euclidean distance of test data instances to all training data instances and chooses instances with the highest distances. 4) Most Uncertain [42]: Ranks the instances in the test dataset by increasing order of the prediction confidence as assigned by the scene classification model. 5) UUB [27]: Combines clustering and the bandit algorithm to query an Oracle. Least Average Similarity and Least Maximum Similarity are popular outlier detection methods; Most Uncertain is similar to the uncertain sampling strategy used in active learning; and UUB is the state of the art unknown unknowns detection method. Apart from those, we further compare with variations of our own framework considering only output from the `REALLY-KNOWS` task, and those with other baseline representation learning and data sampling methods.

Evaluation Metrics. For effectiveness evaluation, we use Precision and Recall to measure the performance on unknown unknowns identification. We consider detection performance in both cases when we are sure the unknown unknowns happen due to the injected data biases and in the entire test set.

Crowdsourcing. We crowdsourced 300 images from each dataset, selected by our feature space partitioning method. We present the same set of images for both the `SHOULD-KNOW` and `REALLY-KNOWS` tasks. For each task, we recruited 300 workers on Prolific[2]. For quality control, only workers whose approval rate was greater than 90% were considered as qualified; to avoid learning bias between the two tasks, each worker is allowed to perform only a single task throughout the entire experiment. The authors manually examined the quality of worker annotations on a random sample, which was found satisfying. Each worker was paid 1.15 USD (0.8 GBP) for participating in our study, translating to an average hourly reward of 10.25 USD (7.41 GBP).

[2]https://www.prolific.co

5.2 Scalpel-HS Performance

Effectiveness. Table 2 reports the performance of comparison methods on detecting unknown unknown images.

We observe that among the baselines, Most Uncertain, which is widely used in detecting known unknowns, yields low performance (similar to Random), providing evidence for the important difference between the problems of detecting known unknowns and unknown unknowns. Among the two outlier detection methods, Least Average Similarity generally outperforms Least Maximum Similarity, indicating that unknown unknowns are distant to the general image population in the feature space. UUB, which considers model confidence, gives better performance than all the other baseline methods, showing that unknown unknowns are related to not only the data but also what models have learned from the data. Most importantly, our proposed framework **Scalpel-HS** achieves the best performance across all settings (unknown unknown types, datasets, and metrics), and outperforms UUB by a significant margin of 31% in F1-score, a strong evidence demonstrating the effectiveness of our framework in unknown unknowns detection.

The relative detection performance of **Scalpel-HS** on the two types of unknown unknowns (False Positive vs. False Negative) is consistent across datasets given the same model; similarly, it is consistent across models given the same dataset. Those results show the robustness of our framework in unknown unknowns detection.

Informativeness. To gain a deeper understanding of the informativeness of unknown unknowns characterization provided by **Scalpel-HS**, we report in Table 3 its performance on uncovering the exact reasoning of the model on unknown unknown images. We observe that our framework successfully exposes the characteristics of all manually created unknown unknowns (except FP3 on MIT67, which corresponds to 13 images only), showing the strong characterizing power of our framework for unknown unknowns. We find a large variability of the performance in detecting unknown unknown images with different characteristics, showing the specificity of unknowns characteristics for detection. As a remark, we note there is a discrepancy between the overall performance in Table 3 and Table 2; this is due to the presence of "natural" unknown unknowns that are not manually induced.

Table 3: `Scalpel-HS` Performance in uncovering ResNet reasoning on unknown unknown images (FP = False Positive, FN = False Negative, # = the number of corresponding unknown unknown).

Type	Index	PLACES				MIT67			
		#	P	R	F	#	P	R	F
FP	FP1	488	0.896	0.588	0.710	158	0.769	0.443	0.562
	FP2	618	0.939	0.629	0.753	545	0.636	0.366	0.465
	FP3	9	0.16	0.111	0.13	13	0.0	0.0	0.0
	All	1115	0.914	0.607	0.729	716	0.666	0.384	0.487
FN	FN1	45	0.531	0.377	0.441	330	0.628	0.472	0.539
	FN2	60	0.275	0.5	0.355	90	0.755	0.453	0.566
	FN3	162	0.721	0.623	0.668	166	1	0.282	0.440
	FN4	98	1	1	1	76	0.709	0.549	0.619
	FN5	16	0.086	0.25	0.129	207	0.166	0.052	0.08
	FN6	47	0.095	0.148	0.116	66	0.755	0.486	0.592
	All	428	0.516	0.600	0.555	880	0.672	0.455	0.543

Table 4: Examples of "natural" unknown unknowns identified by `Scalpel-HS` for ResNet. Note that False Positive is defined w.r.t. Predicted Class and False Negative is defined w.r.t. True Class.)

Type	True Class	Concept	Predicted Class
False Positive	`Hospital Room`	(+)*sink*, (+)*counter*	`Bathroom`
False Negative	`Kitchen`	(-)*oven*, (-)*counter*	`Bathroom`
	`Conference Room`	(-)*chair at table*	`Kitchen`

We show in Table 4 a few those additional unknown unknowns exposed by our framework, i.e., those that are not manually induced. Those characterizations provide easy-to-understand reasons for model failures in unknown unknowns and are thus highly useful for identifying similar errors. In our experiment, they allow us to detect 19% extra False Positive natural unknown unknowns, and 38% extra False Negative natural unknown unknowns.

We show examples of manually induced unknown unknowns detected by our framework in Appendix A.5 and more (including natural ones) in the companion page.

Cost-Efficiency. Figure 5 depicts the performance of **`Scalpel-HS`** under different budgets. As expected the precision decreases and recall increases when the budget increases; yet, we observe that the decrease in precision is much slower than the increase in recall. With 300 images annotated, accounting for 3% of the overall test images in PLACES and 20% of the unknown unknowns with the identified characteristics, we reach a recall of over 60% of all the unknown unknowns; on MIT67, the 300 annotated images account for 9% of the overall test images and 19% of the unknown unknowns with the identified characteristics, we reach a recall of 42%. Those results show that our framework allows to detect **2x** to **3x** unknown unknowns w.r.t. a given budget, demonstrating that our framework is highly cost-efficient.

5.3 Contribution by Automatic Components

We now evaluate the contribution of our representation learning and image sampling methods. Figures 6 (a,b) compare the performance of our framework with our proposed semantically-rich representation learning method and the method with visual features only for representation learning (ResNet152 pre-trained on ImageNet and fine-tuned on our dataset, the rest components of the framework kept the same). The result shows that our proposed

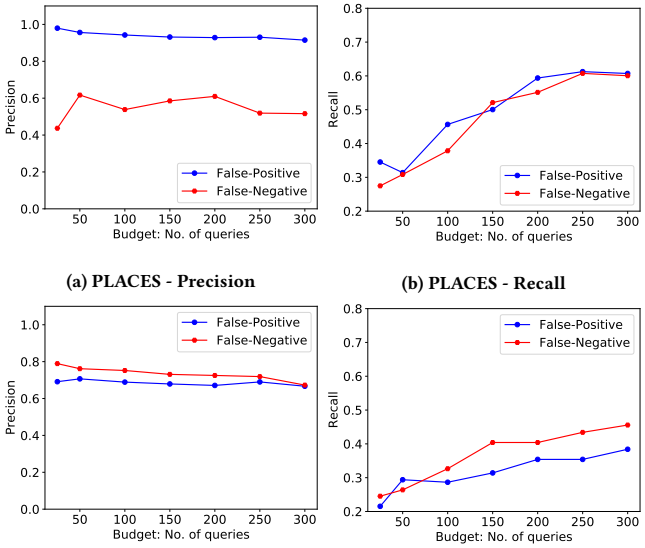

(a) PLACES - Precision (b) PLACES - Recall

(c) MIT67 - Precision (d) MIT67 - Recall

Figure 5: Performance of our framework on unknown unknowns detection for ResNet under different budgets.

representation learning method is a better approach in both precision and recall across almost all budgets, signifying the utility of semantic features in the images for image sampling, and ultimately for unknown unknowns characterization and detection.

Figures 6 (c,d) compare the performance of our framework with our proposed semantic space partitioning (SSP) and other baseline data partitioning or sampling methods. These include: 1) Random Sampling; 2) DSP [27]: optimizes the overall distances within data partitions (minimization) and across partitions (maximization), and then randomly sample representative images. 3) K-means: generates clusters and the nearest instance to the center of each cluster (mean) is selected as the anchor of that partition. We observe that SSP achieves much higher precision with comparable recall (higher when the budget increases), showing the superiority of our partitioning methods in sampling representative unknown unknowns and the effectiveness of joint partitioning and sampling.

5.4 Impacts of `SHOULD-KNOW` and `REALLY-KNOWS`

We evaluate the effect of including human annotations, and in particular, human specification of what a model should know, by comparing the following configurations of our framework: 1) no human task, 2) including only the `REALLY-KNOWS` task, and 3) including both the `REALLY-KNOWS` and `SHOULD-KNOW` tasks.

Figure 7 compares the performance of those configurations under different budgets. We observe that involving human annotations has a big impact on the precision under any budget. In addition, we observe that integrating human annotations has more impact on the recall as the budget increases. Compared to the version of no human tasks, our framework improves by 26% and 10% in precision and recall, respectively (budget=300). Compared to `REALLY-KNOWS` only, with `SHOULD-KNOW` the performance of **`Scalpel-HS`** improves by 5% in both precision and recall. We also notice that the `SHOULD-KNOW` task is especially useful for precise identification of unknown unknowns when the budget is low.

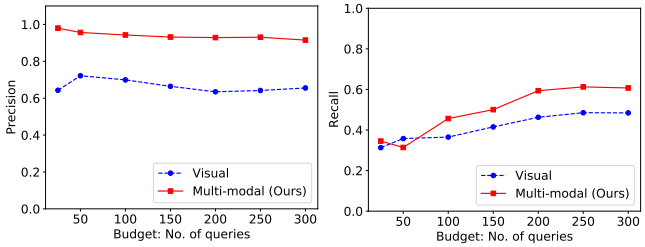

(a) RL - Precision (b) RL - Recall

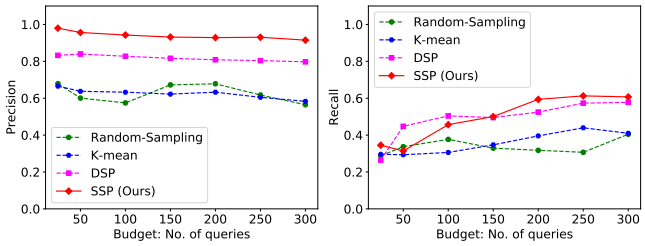

(c) SSP - Precision (d) SSP - Recall

Figure 6: Comparing the effects of our proposed representation learning (RL) and data sampling (SSP) with baseline methods on the performance of our framework under different budgets. Results are obtained on ResNet on the PLACES dataset.

6 RELATED WORK

Unknown Unknowns. Errors of machine learning fall into two broad categories, namely *known unknowns* and *unknown unknowns*, denoting low- and high-confidence errors, respectively. Known unknowns have been extensively studied in the literature of active learning [42]. A set of data sampling strategies have been introduced e.g., query-by-committee [43], uncertainty sampling [28], expected error reduction [39]. More recent development concerns with the dynamic selection of optimal strategies in the training process [7, 9, 21]. All those strategies rely on information provided by the model, thus are not suitable for the identification of unknown unknowns that the model is unaware of.

Unknown unknowns are drawing increasing attention recently due to the criticality for safety and user trust in high-stakes applications. A seminal work by Attenberg *et al.* [5] proposes to ask humans to gather publicly accessible instances that are potentially difficult for a model to handle. This approach has been recently extended by enabling humans access to more information sources to improve the efficiency of unknown unknowns detection. For example, Lakkaraju *et al.* [27] assume human accessibility to the data and introduce a bandit algorithm to exploit data similarity for faster detection. Vandenhof *et al.* [49] on the other hand assume accessibility to model parameters and propose to engage human contributors to generate instances that contradict model reasoning. Most work so far has focused only on the detection task, with the exception of Liu *et al.* [29] that propose to identify the "pattern" of unknown unknowns *for detection*, bringing implicitly the task of unknown unknowns characterization to the horizon. Yet their work does not study characterization on its own—e.g., effectiveness or informativeness. To the best of our knowledge, we are the first to present a focused study on unknown unknowns characterization, considering the roles of humans in both requirement specification

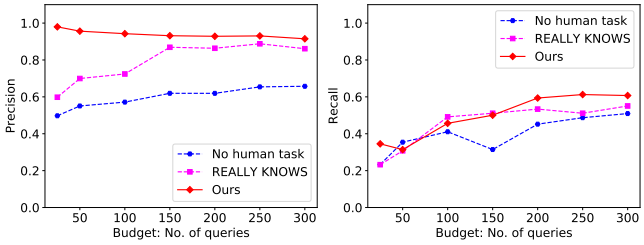

Figure 7: Impacts of human tasks on the performance of our framework under different budgets.

and machine learning behavior interpretation, supported by automatic computational methods for scaling out human contributions.

Automatic and Human Methods. Unknown unknowns arise from biases in the training data. As such, methods developed for outlier detection are relevant for unknown unknowns detection. Typical methods can be characterized as either parametric [1, 2] or non-parametric [13–15] i.e., with or without assumptions on the underlying data distributions. In unknown unknowns detection, outlier detection methods are limited in that 1) they assume the accessibility to the reference data (i.e., training data) which is not necessarily available as in our setting, and 2) they do not take into account what a model has learned thus is limited to identifying model unknowns as we have shown in our experiment.

Another closely related line of work is human-in-the-loop (HItL) machine learning, where human intelligence has been leveraged to address inherent limitations of ML such as reliability and interpretability. Early work in HItL methods mainly focuses on leveraging human intelligence for data labeling [10, 37]. More recent work has investigated the advantage of human computation in debugging ML system components [33] and in identifying biases and noisy labels in the data [22, 51]. The most closely related work, as we discussed, is Lakkaraju *et al.* [27] and Liu *et al.* [29] that use HItL methods for unknown unknowns detection. Recent work that has directly inspired ours is Balayn *et al.* [6] that propose to use human computation to interpret the behavior of image classifiers by attaching semantic concepts to the saliency maps of classification. We employ this method for unknown unknowns characterization in image recognition, and take a step further to show that by including human specified requirements of what a model should know, we can significantly improve unknown unknowns characterization.

7 CONCLUSION

We presented **`Scalpel-HS`**, a human-in-the-loop, semantic analysis framework for characterizing and detecting unknown unknowns of image recognition models. It involves human contributors to specify both what the model should know and describe what it really knows, while minimizing the cognitive load of the tasks leveraging scene graph extraction and machine learning interpretability techniques. It scales out human contributions through both a new semantically-rich representation learning and data sampling method. Our extensive evaluation on multiple models and datasets with different types of unknown unknowns demonstrates that characterizations provided by **`Scalpel-HS`** are not only informative but also highly effective and cost-efficient for unknown unknowns detection.

REFERENCES

[1] Bovas Abraham and George EP Box. 1979. Bayesian analysis of some outlier problems in time series. *Biometrika* 66, 2 (1979), 229–236.

[2] Deepak Agarwal. 2007. Detecting anomalies in cross-classified streams: a bayesian approach. *Knowledge and information systems* 11, 1 (2007), 29–44.

[3] Miltiadis Allamanis, Pankajan Chanthirasegaran, Pushmeet Kohli, and Charles Sutton. 2017. Learning continuous semantic representations of symbolic expressions. In *International Conference on Machine Learning*. PMLR, 80–88.

[4] Saleema Amershi, Max Chickering, Steven M Drucker, Bongshin Lee, Patrice Simard, and Jina Suh. 2015. Modeltracker: Redesigning performance analysis tools for machine learning. In *Proceedings of the 33rd Annual ACM Conference on Human Factors in Computing Systems*. 337–346.

[5] Josh M Attenberg, Pagagiotis G Ipeirotis, and Foster Provost. 2011. Beat the machine: Challenging workers to find the unknown unknowns. In *Workshops at the Twenty-Fifth AAAI Conference on Artificial Intelligence*.

[6] Agathe Balayn, Panagiotis Soilis, Christoph Lofi, Jie Yang, and Alessandro Bozzon. 2021. What do You Mean? Interpreting Image Classification with Crowdsourced Concept Extraction and Analysis. In *Proceedings of the Web Conference 2021*. 1937–1948.

[7] Yoram Baram, Ran El-Yaniv, and Kobi Luz. 2004. Online Choice of Active Learning Algorithms. *Journal of Machine Learning Research* 5 (Dec. 2004), 255–291.

[8] Varun Chandola, Arindam Banerjee, and Vipin Kumar. 2007. Outlier detection: A survey. *Comput. Surveys* 14 (2007), 15.

[9] Hong-Min Chu and Hsuan-Tien Lin. 2016. Can Active Learning Experience Be Transferred? *IEEE 16th International Conference on Data Mining* (2016), 841–846.

[10] Jia Deng, Wei Dong, Richard Socher, Li-Jia Li, Kai Li, and Li Fei-Fei. 2009. Imagenet: A large-scale hierarchical image database. In *2009 IEEE conference on computer vision and pattern recognition*. IEEE, 248–255.

[11] Mengnan Du, Ninghao Liu, and Xia Hu. 2019. Techniques for interpretable machine learning. *Commun. ACM* 63, 1 (2019), 68–77.

[12] Alexander Erlei, Franck Nekdem, Lukas Meub, Avishek Anand, and Ujwal Gadiraju. 2020. Impact of Algorithmic Decision Making on Human Behavior: Evidence from Ultimatum Bargaining. In *Proceedings of the AAAI Conference on Human Computation and Crowdsourcing*, Vol. 8. 43–52.

[13] Eleazar Eskin. 2000. Anomaly Detection over Noisy Data using Learned Probability Distributions. In *Proceedings of the Seventeenth International Conference on Machine Learning*. 255–262.

[14] Eleazar Eskin, Andrew Arnold, Michael Prerau, Leonid Portnoy, and Sal Stolfo. 2002. A geometric framework for unsupervised anomaly detection. In *Applications of data mining in computer security*. Springer, 77–101.

[15] Tom Fawcett and Foster Provost. 1997. Adaptive fraud detection. *Data mining and knowledge discovery* 1, 3 (1997), 291–316.

[16] Chris Fields. 2016. How Humans Recognize Objects: Segmentation, Categorization and Individual Identification. *Frontiers in psychology* 7 (2016), 400.

[17] Ujwal Gadiraju and Jie Yang. 2020. What can crowd computing do for the next generation of AI systems?. In *2020 Crowd Science Workshop: Remoteness, Fairness, and Mechanisms as Challenges of Data Supply by Humans for Automation*. 7–13.

[18] Wenzhong Guo, Jianwen Wang, and Shiping Wang. 2019. Deep multimodal representation learning: A survey. *IEEE Access* 7 (2019), 63373–63394.

[19] Kaiming He, Xiangyu Zhang, Shaoqing Ren, and Jian Sun. 2016. Deep residual learning for image recognition. In *Proceedings of the IEEE conference on computer vision and pattern recognition*. 770–778.

[20] Martin N Hebart, Charles Y Zheng, Francisco Pereira, and Chris I Baker. 2020. Revealing the multidimensional mental representations of natural objects underlying human similarity judgements. *Nature Human Behaviour* 4, 11 (2020).

[21] Wei-Ning Hsu and Hsuan-Tien Lin. 2015. Active Learning by Learning. In *Proceedings of the Twenty-Ninth AAAI Conference on Artificial Intelligence*.

[22] Xiao Hu, Haobo Wang, Anirudh Vegesana, Somesh Dube, Kaiwen Yu, Gore Kao, Shuo-Han Chen, Yung-Hsiang Lu, George K Thiruvathukal, and Ming Yin. 2020. Crowdsourcing Detection of Sampling Biases in Image Datasets. In *Proceedings of The Web Conference 2020*. 2955–2961.

[23] Gao Huang, Zhuang Liu, Laurens Van Der Maaten, and Kilian Q Weinberger. 2017. Densely connected convolutional networks. In *Proceedings of the IEEE conference on computer vision and pattern recognition*. 4700–4708.

[24] Thomas N. Kipf and Max Welling. 2017. Semi-Supervised Classification with Graph Convolutional Networks. In *Intl. Conf. on Learning Representations*.

[25] David R Krathwohl. 2002. A revision of Bloom's taxonomy: An overview. *Theory into practice* 41, 4 (2002), 212–218.

[26] Alex Krizhevsky, Ilya Sutskever, and Geoffrey E Hinton. 2012. Imagenet classification with deep convolutional neural networks. *Advances in neural information processing systems* 25 (2012), 1097–1105.

[27] Himabindu Lakkaraju, Ece Kamar, Rich Caruana, and Eric Horvitz. 2017. Identifying unknown unknowns in the open world: representations and policies for guided exploration. In *Proceedings of the Thirty-First AAAI Conference on Artificial Intelligence*. 2124–2132.

[28] David D. Lewis and William A. Gale. 1994. A Sequential Algorithm for Training Text Classifiers. In *Proceedings of the 17th Annual International ACM SIGIR Conference on Research and Development in Information Retrieval*. 3–12.

[29] Anthony Liu, Santiago Guerra, Isaac Fung, Gabriel Matute, Ece Kamar, and Walter Lasecki. 2020. Towards Hybrid Human-AI Workflows for Unknown Unknown Detection. In *Proceedings of The Web Conference 2020*. 2432–2442.

[30] Eric Margolis and Stephen Laurence. 2007. The ontology of concepts-abstract objects or mental representations? *Noûs* 41, 4 (2007), 561–593.

[31] Sina Mohseni, Jeremy E Block, and Eric D Ragan. 2021. Quantitative Evaluation of Machine Learning Explanations: A Human-Grounded Benchmark. (2021).

[32] Nicolò Navarin, Dinh Van Tran, and Alessandro Sperduti. 2019. Universal Readout for Graph Convolutional Neural Networks. In *2019 International Joint Conference on Neural Networks*. 1–7.

[33] Besmira Nushi, Ece Kamar, Eric Horvitz, and Donald Kossmann. 2017. On human intellect and machine failures: Troubleshooting integrative machine learning systems. In *Thirty-First AAAI Conference on Artificial Intelligence*.

[34] Jeffrey Pennington, Richard Socher, and Christopher D. Manning. 2014. GloVe: Global Vectors for Word Representation. In *Empirical Methods in Natural Language Processing*. 1532–1543.

[35] Iyad Rahwan, Manuel Cebrian, Nick Obradovich, Josh Bongard, Jean-François Bonnefon, Cynthia Breazeal, Jacob W Crandall, Nicholas A Christakis, Iain D Couzin, Matthew O Jackson, et al. 2019. Machine behaviour. *Nature* 568, 7753 (2019), 477–486.

[36] Bing Ran and P Robert Duimering. 2010. Conceptual combination: Models, theories and controversies. *International Journal of Cognitive Linguistics* 1, 1 (2010), 65–90.

[37] Vikas C Raykar, Shipeng Yu, Linda H Zhao, Gerardo Hermosillo Valadez, Charles Florin, Luca Bogoni, and Linda Moy. 2010. Learning from crowds. *Journal of Machine Learning Research* 11, 4 (2010).

[38] Shaoqing Ren, Kaiming He, Ross Girshick, and Jian Sun. 2016. Faster r-cnn: Towards real-time object detection with region proposal networks. *IEEE transactions on pattern analysis and machine intelligence* 39, 6 (2016), 1137–1149.

[39] Nicholas Roy and Andrew McCallum. 2001. Toward Optimal Active Learning Through Sampling Estimation of Error Reduction. In *ICML*. 894–905.

[40] Keisuke Sakaguchi, Ronan Le Bras, Chandra Bhagavatula, and Yejin Choi. 2020. Winogrande: An adversarial winograd schema challenge at scale. In *Proceedings of the AAAI Conference on Artificial Intelligence*, Vol. 34. 8732–8740.

[41] Nithya Sambasivan, Shivani Kapania, Hannah Highfill, Diana Akrong, Praveen Kumar Paritosh, and Lora Mois Aroyo. 2021. "Everyone wants to do the model work, not the data work": Data Cascades in High-Stakes AI. (2021).

[42] Burr Settles. 2012. Active learning. *Synthesis lectures on artificial intelligence and machine learning* 6, 1 (2012), 1–114.

[43] H. S. Seung, M. Opper, and H. Sompolinsky. 1992. Query by Committee. In *Proceedings of the Fifth Annual Workshop on Computational Learning Theory* (Pittsburgh, Pennsylvania, USA). 287–294.

[44] Herbert A. Simon. 1979. *Models of thought*. Vol. 352. Yale university press.

[45] Karen Simonyan, Andrea Vedaldi, and Andrew Zisserman. 2013. Deep inside convolutional networks: Visualising image classification models and saliency maps. *arXiv preprint arXiv:1312.6034* (2013).

[46] Daniel Smilkov, Nikhil Thorat, Been Kim, Fernanda Viégas, and Martin Wattenberg. 2017. Smoothgrad: removing noise by adding noise. *arXiv:1706.03825* (2017).

[47] Fan-Yun Sun, Jordan Hoffman, Vikas Verma, and Jian Tang. 2019. InfoGraph: Unsupervised and Semi-supervised Graph-Level Representation Learning via Mutual Information Maximization. In *International Conference on Learning Representations*.

[48] Christian Szegedy, Sergey Ioffe, Vincent Vanhoucke, and Alexander Alemi. 2017. Inception-v4, inception-resnet and the impact of residual connections on learning. In *Proceedings of the AAAI Conference on Artificial Intelligence*, Vol. 31.

[49] Colin Vandenhof. 2019. A Hybrid Approach to Identifying Unknown Unknowns of Predictive Models. In *Proceedings of the AAAI Conference on Human Computation and Crowdsourcing*, Vol. 7. 180–187.

[50] Jiaxuan Wang, Jeeheh Oh, Haozhu Wang, and Jenna Wiens. 2018. Learning credible models. In *Proceedings of the 24th ACM SIGKDD International Conference on Knowledge Discovery & Data Mining*. 2417–2426.

[51] Jie Yang, Alisa Smirnova, Dingqi Yang, Gianluca Demartini, Yuan Lu, and Philippe Cudré-Mauroux. 2019. Scalpel-cd: leveraging crowdsourcing and deep probabilistic modeling for debugging noisy training data. In *WWW*. 2158–2168.

[52] Rex Ying, Jiaxuan You, Christopher Morris, Xiang Ren, William L Hamilton, and Jure Leskovec. 2018. Hierarchical graph representation learning with differentiable pooling. *arXiv preprint arXiv:1806.08804* (2018).

[53] Rowan Zellers, Mark Yatskar, Sam Thomson, and Yejin Choi. 2018. Neural Motifs: Scene Graph Parsing with Global Context. In *Conference on Computer Vision and Pattern Recognition*.

[54] Zijian Zhang, Jaspreet Singh, Ujwal Gadiraju, and Avishek Anand. 2019. Dissonance between human and machine understanding. *Proceedings of the ACM on Human-Computer Interaction* 3, CSCW (2019), 1–23.

[55] Bolei Zhou, Agata Lapedriza, Jianxiong Xiao, Antonio Torralba, and Aude Oliva. 2014. Learning deep features for scene recognition using places database. (2014).

A APPENDIX

A.1 Learning Image Representations

To obtain graph-level representations, we train the graph encoder end-to-end using the approach proposed by Sun et al. [47], by maximizing the mutual information between graph-level and patch-level representations. The patch-level representation refers to the representation of nodes learned by aggregating the features of their neighborhood nodes, at the last GCN layer, while the graph-level representation is a fixed length vector obtained by pooling all patch-level representations. To train our graph encoder, we define the following objective function:

$$max \frac{1}{|G|} \sum_{g \in G} \left[\frac{1}{|g|} \sum_{i=1}^{|g|} D\left(\vec{U}_i, \vec{U}_g\right) \right]$$

where $|G|$ is the number of graphs in train set, $|g|$ is the number of nodes in graph g, and $\vec{U}_i$, $\vec{U}_g$ are representations of node i and graph g, respectively. D denotes a mutual information estimator which is modeled as a discriminator to score the agreement between patch-level and graph-level representations. The agreement score is obtained by simply computing the dot product between two representations.

Hyperparameter Setting. The number of GNN layers are chosen from $\{4, 8, 12\}$. Initial learning rate is chosen from the set $\{0.01, 0.001, 0.0001\}$. We set the batch size to 64. The number of epochs are chosen from $\{30, 60, 90\}$.

A.2 Semantic Space Partitioning Algorithm

The input of our GA-based method is a set of data points $\mathcal{D} = \{d_1, d_2, ..., \}$ where each d_i consists of (feature vector, weighted concept) pairs, and the number of representative samples $\mathcal{B}$ to be found. Note that the number of generated partitions is equal to the number of representative samples. We initialize the genetic algorithm by constructing a population of random chromosomes $\mathcal{P} = \{p_1, p_2, ..., \}$, where each chromosome p_i consists of $\mathcal{B}$ candidate samples. Algorithm 1 implements the fitness function, which corresponds to the proposed objective function (See Eq.4). The fitness function guides the exploration through the search space towards an optimal solution.

GAs are prone to premature convergence to local optima. Inspired by [40], we address this problem by adjusting the mutation rate (Pm) while the algorithm explores the search space. To avoid the generation of invalid solutions and to improve the performance of the GA, we use a greedy approach to the mutation process, which mutates the offspring only if the mutated solution gains lower fitness value.

Hyperparameter Setting. Population, elitism, mutation-rate and cross-over rate are regarded as hyper parameters, and therefore can be found via grid search ($N \in \{50, 100, 150, 200\}$; elitism $E \in \{5, 10, 15, 20, 30\}$; mutation rate $P_m \in \{0.0005, 0.001, 0.005, 0.01, 0.05\}$; and cross-over rate $P_c \in \{0.5, 0.6, 0.7, 0.8, 0.9\}$). We set $N = 100$; $E = 20\%$; $P_m = 0.005$; $and P_c = 0.7$. We used a stagnation based termination criterion; following [3], we terminate the algorithm after $\sqrt[2]{\mathcal{B}}$ generations, where $\mathcal{B}$ denotes the number of representative samples to be found, and $\mathcal{D}$ is the number of data points.

Algorithm 1 Fitness algorithm

```
procedure FITNESS(R, D, F, W)
    fitness ← 0
    for d ∈ D do
        max_similarity ← ∞
        for r ∈ R do
            f_r ← GetWeightedFeatures(F, W, r)
            f_d ← GetFeatures(F, d)
            similarity ← Cosine(f_r, f_d)
            if similarity ≤ max_similarity then
                max_similarity ← similarity
            end if
        end for
        fitness ← fitness + max_similarity
    end for
    return fitness
end procedure
```

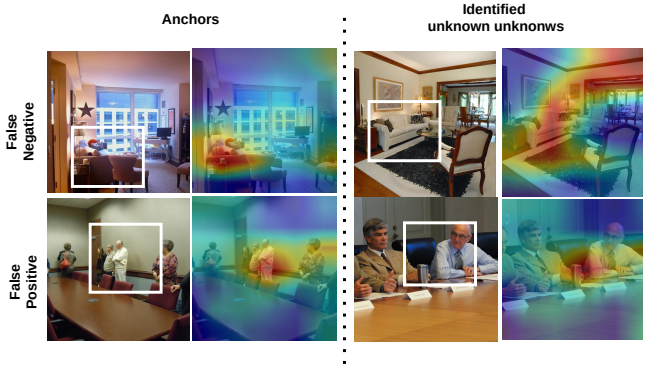

Figure 8: Example of unknown unknowns characterized and detected by `Scalpel-HS`: (upper-row) False Negative <`Living room`, (-)*sofa*, `Dorm room`> and (lower-row) False Positive <`Conference room`, (+)*person*, `Kindergarden`>. For each case, we show the sampled representative image with relevant concepts on the left and an additional similar unknown unknown image on the right. All images are shown together with a corresponding saliency map showing where the model is attending to in making the incorrect prediction. Note that in the False Negative case, the sofa leads to False Negative w.r.t. `Living Room` yet False Positive w.r.t. `Dorm Room`.

A.3 Annotation Workflow in Large Figures

Figures 9 and 10 show the zoomed version of our `SHOULD-KNOW` and `REALLY-KNOWS` human computation tasks.

A.4 Experimental Setup Details

We filter the two datasets by keeping images of the following scene classes: *dining room, bathroom, conference room, kindergarden, hospital room, kitchen, living room, bedroom, dorm room.*

A.5 Examples of Unknown Unknowns Identified by `Scalpel-HS`

We show a few examples of unknown unknown images **`Scalpel-HS`** identified and characterized, for both False Positive and False Negative. Figure 8 illustrates two characterizations of each type for both the sampled images (i.e., anchors) two similar ones detected by our framework.

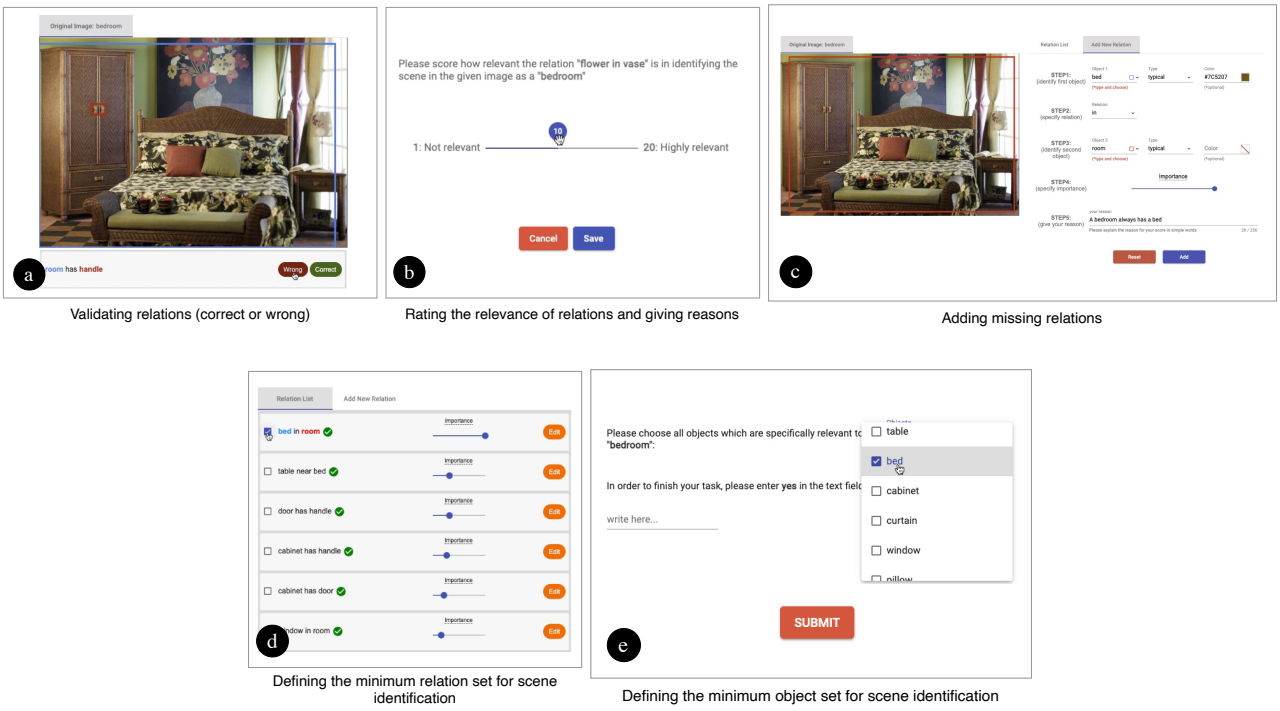

Figure 9: The procedure of the SHOULD-KNOW task zoomed.

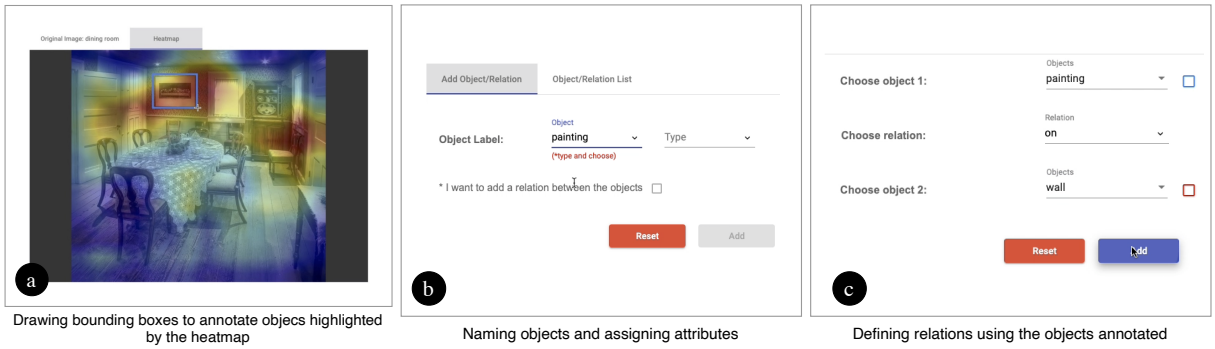

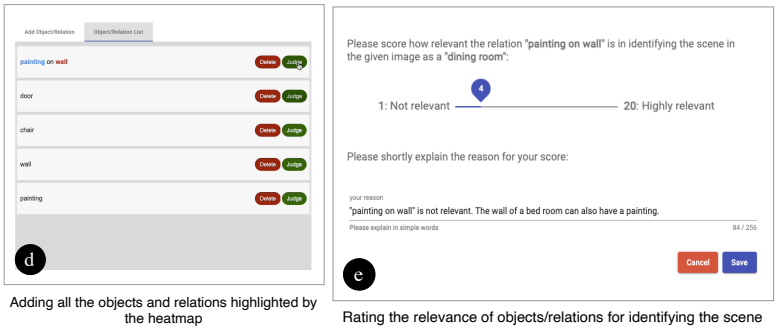

Figure 10: The procedure of the REALLY-KNOWS task zoomed.